Magnetic field of a cylindrical coil

Velimir Labinac, Nataša Erceg, and Dubravka Kotnik-Karuza

Citation: American Journal of Physics **74**, 621 (2006); doi: 10.1119/1.2198885
View online: https://doi.org/10.1119/1.2198885
View Table of Contents: http://aapt.scitation.org/toc/ajp/74/7
Published by the American Association of Physics Teachers

Magnetic field of a cylindrical coil

Velimir Labinac, Nataša Erceg, and Dubravka Kotnik-Karuza[a)]
Department of Physics, Faculty of Arts and Sciences, Rijeka, Omladinska 14, Rijeka 51000, Croatia

(Received 17 August 2005; accepted 31 March 2006)

We calculate the magnetic fields of cylindrical coils due to a surface current and a volume current and compare our theoretical results to measured magnetic fields of two coil types: single-layer solenoid and cylindrical thick coil by a simple experimental apparatus. Good agreement is found with the theoretical results. © *2006 American Association of Physics Teachers.*
[DOI: 10.1119/1.2198885]

I. INTRODUCTION

The calculation of static magnetic fields is often introduced for an infinite solenoid, which produces a constant nonzero magnetic field inside and a zero field outside the solenoid. However, a general solution of the magnetic field distribution for a finite solenoid, despite its practical importance, is not covered in most textbooks.

Textbooks and papers with a pedagogical emphasis concentrate on a simple determination of the magnetic field of an infinite solenoid,[1–5] or on some special cases of the field of a finite solenoid (for example, the field along the axis and the field just outside of it).[6–9] Other papers are concerned with purely numerical and/or analytical calculation of the magnetic field of axisymmetric currents appearing in various coil designs.[10–12] The number of papers that discuss experimental determination of different magnetic field configurations is small.[13–15]

In this paper we discuss the magnetic field of a coil using both theory and experiment. We present a method for the calculation of the magnetic fields of cylindrical coils and obtain analytical expressions for two basic coil types: a thin solenoid and a thick coil.

We will use the term *coil* as a general expression for real configurations, *loop*, one turn of wire, *solenoid*, a coil with arbitrary cross section and length greater than its diameter, and *thick coil*, a coil with cylindrical geometry and wound wire forming a thick layer of the same order of magnitude as the inner radius of the coil.

II. MODELS

We will use cylindrical coordinates in the half-space $z \geqslant 0$ and model an iron-free thin solenoid and thick coil by a cylindrical surface current and cylindrical shell volume current, respectively. The origin of cylindrical coordinates is taken at the axis of the coil with $z=0$ at its end. We initially will use Bessel functions in our calculations although other functions, such as Legendre functions and polynomials,[16–18] could have been applied as well. The integrals appearing in the calculations are listed in the Appendix.

A. Cylindrical surface current

A current loop $\boldsymbol{C}$ of radius a carrying current I is located parallel to the plane xy, its center being on the z axis [see Fig. 1(a)]. The vector potential of the loop is

$$\mathbf{A}(\mathbf{x}) = \frac{\mu_0 I}{4\pi}\oint_C \frac{d\mathbf{l}'}{|\mathbf{x}-\mathbf{x}'|}, \tag{1}$$

where μ_0 is the permeability of free space and $d\mathbf{l}' = a d\phi' \mathbf{e}_\phi$. The unit vector $\mathbf{e}_\phi$ is oriented in the positive sense of the polar angle ϕ. The integral in Eq. (1) can be calculated by a series expansion of $|\mathbf{x}-\mathbf{x}'|^{-1}$ in terms of the Bessel functions $J_m(\xi)$:[19]

$$\frac{1}{|\mathbf{x}-\mathbf{x}'|} = \sum_{m=-\infty}^{\infty}\int_0^\infty dk e^{im(\phi-\phi')} J_m(k\rho) J_m(ka) e^{-k|z-z'|}. \tag{2}$$

The magnitude of the vector potential is independent of ϕ because of the azimuthal symmetry of the currents.

After integration with respect to ϕ', only terms with indices $m=-1,1$ remain in the sum. By using the identity $J_{-1}(\xi) = -J_1(\xi)$, the x component of the potential vanishes and the vector potential becomes

$$\mathbf{A}(\rho,z) = \frac{\mu_0 I a}{2}\mathbf{e}_y \int_0^\infty dk J_1(k\rho) J_1(ka) e^{-k|z-z'|}. \tag{3}$$

Equation (3) is obtained for $\phi=0$ with $\mathbf{e}_y = \mathbf{e}_\phi$. Another choice of ϕ would not change the potential. If we take into account that the vector potential has the same direction as the current, we can let $\mathbf{A} = A_\phi \mathbf{e}_\phi$, where

$$A_\phi(\rho,z) = \frac{\mu_0 I a}{2}\int_0^\infty dk J_1(k\rho) J_1(ka) e^{-k|z-z'|}. \tag{4}$$

By use of Eq. (4) and the superposition principle, we can derive the vector potential of an arbitrary cylindrically symmetric current distribution.

If the wire is sufficiently thin, that is, if the radius of the wire is much less than the mean radius of the coil, the coil can be modeled by a cylindrical surface current $\mathbf{K} = K\mathbf{e}_\phi$ with

$$K = \frac{\Delta I}{\Delta z'} = \frac{NI}{L}, \tag{5}$$

where N is the number of turns and L is the cylinder length [Fig. 1(b)]. We use Eq. (4) for a narrow circular strip of width $\Delta z'$ carrying the current ΔI and obtain

$$\Delta A_\phi(\rho,z) = \frac{\mu_0 a}{2}\Delta I \int_0^\infty dk J_1(k\rho) J_1(ka) e^{-k|z-z'|}. \tag{6}$$

We use the superposition principle and obtain the vector potential of the entire cylinder in the limit $\Delta z' \to 0$,

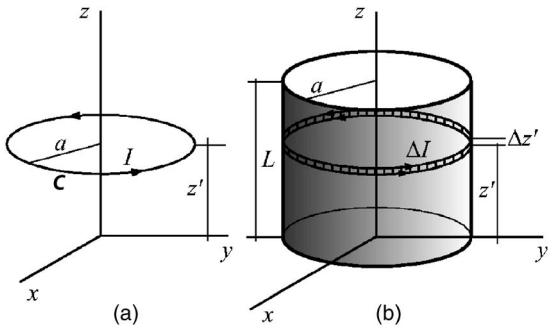

Fig. 1. The geometry of (a) current loop and (b) cylindrical surface current used in Sec. II A.

$$A_\phi(\rho,z)=\frac{\mu_0 aNI}{2L}\int_0^L dz'\int_0^\infty dk J_1(k\rho)J_1(ka)e^{-k|z-z'|}, \quad (7)$$

with one end of the cylinder at $z=0$ and the other at $z=L$. We consider the region $z\geqslant 0$. Integration with respect to z' is straightforward:

$$\int_0^L dz' e^{-k|z-z'|}=k^{-1}f(k;z), \quad (8)$$

where the function $f(k;z)$ is defined by

$$f(k;z)\equiv\begin{cases} e^{-k(z-L)}-e^{-kz}, & z\geqslant L \\ 2-e^{-k(L-z)}-e^{-kz}, & 0\leqslant z<L \end{cases}. \quad (9)$$

The vector potential becomes

$$A_\phi(\rho,z)=\frac{\mu_0 aNI}{2L}\int_0^\infty dk k^{-1}J_1(k\rho)J_1(ka)f(k;z). \quad (10)$$

The magnetic field, corresponding to the potential in Eq. (10), is calculated using $\mathbf{B}=\boldsymbol{\nabla}\times\mathbf{A}$ in cylindrical coordinates:

$$\mathbf{B}=-\frac{\partial A_\phi}{\partial z}\mathbf{e}_\rho+\frac{1}{\rho}\frac{\partial}{\partial\rho}(\rho A_\phi)\mathbf{e}_z. \quad (11)$$

The radial component B_ρ requires the calculation of $\partial f(k,z)/\partial z$, leading to

$$B_\rho=-\frac{\partial A_\phi}{\partial z}=\frac{\mu_0 aNI}{2L}\int_0^\infty dk(e^{-k|z-L|}-e^{-kz})J_1(k\rho)J_1(ka). \quad (12)$$

It is possible to express the integrals in Eq. (12) in terms of Legendre functions of the second kind $Q_{1/2}(\xi)$, or by Gauss hypergeometric functions $F(5/4,3/4;2;\xi^{-2})$ [see Eqs. (A1) and (A2)].[20] The radial magnetic field component is

$$\frac{B_\rho}{B_\infty}=\frac{1}{8}\sqrt{\frac{a}{2\rho}}\left\{\left[\frac{2a\rho}{|z-L|^2+\rho^2+a^2}\right]^{3/2}\times F\left(\frac{5}{4},\frac{3}{4};2;\left[\frac{2a\rho}{|z-L|^2+\rho^2+a^2}\right]^2\right)-\left[\frac{2a\rho}{z^2+\rho^2+a^2}\right]^{3/2}F\left(\frac{5}{4},\frac{3}{4};2;\left[\frac{2a\rho}{z^2+\rho^2+a^2}\right]^2\right)\right\}, \quad (13)$$

where the parameter

$$B_\infty\equiv\frac{\mu_0 NI}{L} \quad (14)$$

represents the magnitude of the magnetic field inside an infinite length solenoid carrying the current I.

For the real coil described in Sec. III, $B_\infty=6.08I$ giving a value of 30.40 G for a current of 5 A. The axial magnetic field component is found by using the Bessel functions identities, $J_1(k\rho)=(k\rho/2)[J_0(k\rho)+J_2(k\rho)]$ and $2J_1'(k\rho)=J_0(k\rho)-J_2(k\rho)$:

$$B_z=\frac{A_\phi}{\rho}+\frac{\partial A_\phi}{\partial\rho}=\frac{\mu_0 aNI}{2L}\int_0^\infty dk J_0(k\rho)J_1(ka)f(k;z). \quad (15)$$

The integral in Eq. (15) can be expanded in a series of Gauss hypergeometric functions. The advantage of a series is that it facilitates the consideration of some limiting cases. Moreover, sometimes a small number of terms are sufficient. MATHEMATICA[21] is much more rapid in plotting functions defined by series than by integrals. A series expansion can be carried out in the regions $\rho<a$ and $\rho>a$ by expanding $J_0(k\rho)$ and $J_1(ka)$, respectively, and then integrating term by term. The integrals (A3) and (A4) from the Appendix have been used. The axial magnetic field component is

$$\frac{B_z(z>L,\rho<a)}{B_\infty}=-\sum_{n=0}^\infty\frac{(-1)^n}{2^{2n+2}}\frac{(2n+1)!}{(n!)^2}\left[\left(\frac{a}{z}\right)^2\left(\frac{\rho}{z}\right)^{2n}F\left(n+1,n+\frac{3}{2};2;-\frac{a^2}{z^2}\right)-\left(\frac{a}{z-L}\right)^2\left(\frac{\rho}{z-L}\right)^{2n}\times F\left(n+1,n+\frac{3}{2};2;-\frac{a^2}{(z-L)^2}\right)\right], \quad (16a)$$

$$\frac{B_z(z>L,\rho>a)}{B_\infty}=-\sum_{n=0}^\infty\frac{(-1)^n}{2^{2n+2}}\frac{(2n+1)!}{n!(n+1)!}\left[\left(\frac{a}{z}\right)^{2n+2}F\left(n+1,n+\frac{3}{2};1;-\frac{\rho^2}{z^2}\right)-\left(\frac{a}{z-L}\right)^{2n+2}F\left(n+1,n+\frac{3}{2};1;-\frac{\rho^2}{(z-L)^2}\right)\right], \quad (16b)$$

$$\frac{B_z(z<L,\rho<a)}{B_\infty}=1-\sum_{n=0}^{\infty}\frac{(-1)^n}{2^{2n+2}}\frac{(2n+1)!}{(n!)^2}\left[\left(\frac{a}{z}\right)^2\left(\frac{\rho}{z}\right)^{2n}F\left(n+1,n+\frac{3}{2};2;-\frac{a^2}{z^2}\right)+\left(\frac{a}{L-z}\right)^2\left(\frac{\rho}{L-z}\right)^{2n}\times F\left(n+1,n+\frac{3}{2};2;-\frac{a^2}{(L-z)^2}\right)\right], \tag{16c}$$

$$\frac{B_z(z<L,\rho>a)}{B_\infty}=-\sum_{n=0}^{\infty}\frac{(-1)^n}{2^{2n+2}}\frac{(2n+1)!}{n!(n+1)!}\left[\left(\frac{a}{z}\right)^{2n+2}F\left(n+1,n+\frac{3}{2};1;-\frac{\rho^2}{z^2}\right)+\left(\frac{a}{L-z}\right)^{2n+2}F\left(n+1,n+\frac{3}{2};1;-\frac{\rho^2}{(L-z)^2}\right)\right]. \tag{16d}$$

To calculate the values of the axial component at the ends of a solenoid, the limits of B_z as $z\to 0$ and $z\to L$ can be derived from Eq. (16).

The advantage of the series representation, Eq. (16), is demonstrated by an example of a field just outside a long finite size solenoid ($L\gg\rho>a$) in its median plane $z=L/2$ where the radial field component is equal to zero. The term with $n=0$ from Eq. (16d) becomes

$$\left(\frac{a}{L}\right)^2F\left(1,\frac{3}{2};1;-\frac{\rho^2}{(L/2)^2}\right)=\left(\frac{a}{L}\right)^2\frac{1}{[1+(2\rho/L)^2]^{3/2}}\simeq\left(\frac{a}{L}\right)^2\left(1-6\frac{\rho^2}{L^2}+\cdots\right). \tag{17}$$

The term with $n=1$ up to the fourth order in a/L and ρ/L is

$$\left(\frac{a}{L}\right)^4F\left(2,\frac{3}{2};\frac{5}{2};-\frac{\rho^2}{(L/2)^2}\right)=\left(\frac{a}{L}\right)^4\frac{1-\frac{3}{2}(2\rho/L)^2}{[1+(2\rho/L)^2]^{7/2}}\simeq\left(\frac{a}{L}\right)^4, \tag{18}$$

leading to the approximate expression

$$B_z\simeq-\frac{2\mu_0NI}{L}\left(\frac{a}{L}\right)^2\left[1-6\left(\frac{\rho}{L}\right)^2-3\left(\frac{a}{L}\right)^2\right]. \tag{19}$$

B. Cylindrical shell volume current

The current density of a cylindrical shell carrying the current NI uniformly distributed across the cross section shown in Fig. 2 is given by

$$\frac{\Delta I}{\Delta S'}=\frac{NI}{(b-a)L}, \tag{20}$$

where N is the number of turns of the thick coil and $\Delta S'=\Delta\rho'\Delta z'$ is the finite surface element. By inserting Eq. (20) into a modified form of Eq. (7), where the single radius a is replaced by an integral over the thick cylindrical shell, we obtain

$$A_\phi=\frac{\mu_0NI}{2(b-a)L}\int_0^L dz'\int_a^b d\rho'\rho'\int_0^\infty dkJ_1(k\rho)J_1(k\rho')e^{-k|z-z'|}. \tag{21}$$

The z' integration is the same as that in Eq. (8), leading again to the function $f(k;z)$ defined in Eq. (9). The ρ' integration is shown in Eq. (A5), leaving a final integral for A_ϕ:

$$A_\phi=\frac{\mu_0NIa^2\pi}{4L(b-a)}\int_0^\infty dkk^{-1}J_1(k\rho)f(k;z)g(k). \tag{22}$$

The function $g(k)$ is given by

$$g(k)\equiv\frac{1}{ka}\left[-J_1(ka)H_0(ka)+\frac{b}{a}J_1(kb)H_0(kb)+J_0(ka)H_1(ka)-\frac{b}{a}J_0(kb)H_1(kb)\right], \tag{23}$$

where $H_0(\xi)$ and $H_1(\xi)$ are Struve functions.[22] The magnetic field is calculated from $\mathbf{A}$ as it was in Sec. II A, giving

$$\frac{B_\rho}{B_\infty}=\frac{a^2\pi}{4(b-a)}\int_0^\infty dkJ_1(k\rho)(e^{-k|z-L|}-e^{-kz})g(k), \tag{24a}$$

$$\frac{B_z}{B_\infty}=\frac{a^2\pi}{4(b-a)}\int_0^\infty dkJ_0(k\rho)f(k;z)g(k). \tag{24b}$$

These two integrals have to be done numerically to obtain the final values for the magnetic field. For the coil used in our experiment, B_∞ defined by Eq. (14) equals 76.74 I giving a magnetic field of 383.70 G for a current of 5 A.

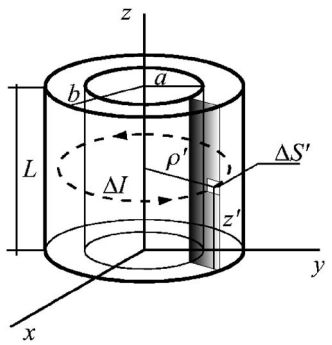

Fig. 2. The geometry of the cylindrical shell volume current used in Sec. II B.

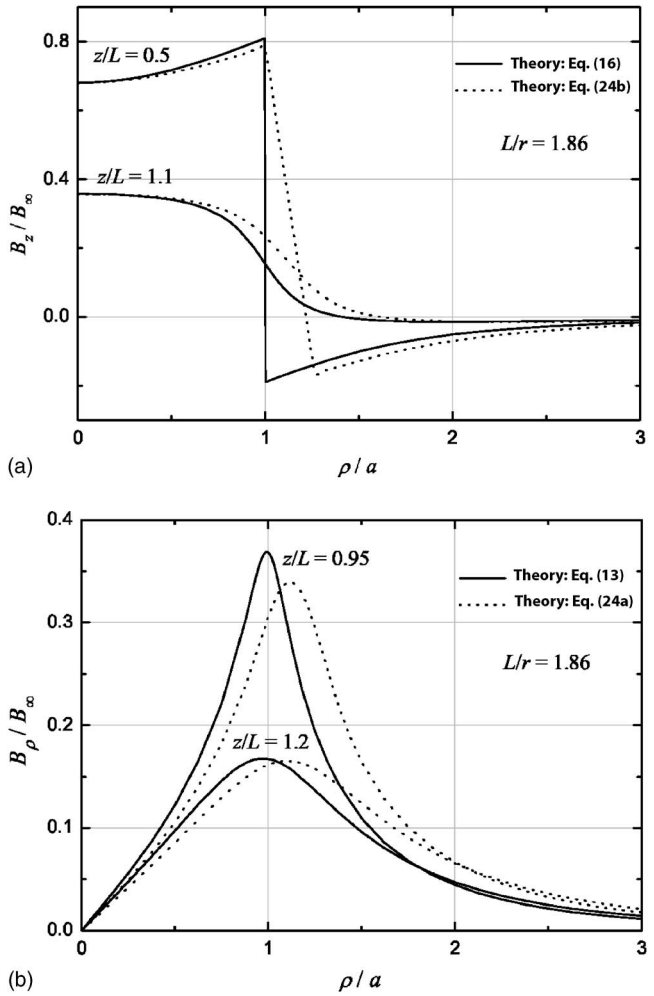

Fig. 3. The computed magnetic field components for the cylindrical surface current, Eqs. (13) and (16), and the cylindrical shell volume current, Eq. (24).

C. Discussion of the field

The radial and axial magnetic field components, Eqs. (13) and (16), and the corresponding magnetic field components in Eq. (24) for coils of equal length, mean radius r, and product NI are plotted in Fig. 3. The parameters of the current carrying layer in Sec. II B are given by $a=115$ mm and $b=150$ mm for our thick coil.

The axial component of the magnetic field in Eq. (16) has a discontinuity in the region $0<z<L$ at $\rho=a$. If $B_{z,1}$ and $B_{z,2}$ represent the axial magnetic field components inside and outside the coil, respectively, the boundary condition at $\rho=a$ is given by

$$-(B_{z,2}-B_{z,1})=\mu_0\frac{NI}{L}. \tag{25}$$

This discontinuity is clearly seen in Fig. 3. The axial magnetic field component in the region $z>L$ is continuous. The axial component of the field in Eq. (24b) in the region $z<L$ is continuous, but not smooth, falling abruptly to zero (with some overshoot) between $\rho=a$ and $\rho=b$.

The radial component in Eq. (13) is continuous everywhere, except for a logarithmic singularity at $\rho=a$ in the boundary planes $z=0$ and $z=L$. The graph in Fig. 3 clearly shows a narrowing of the curve for $z/L=0.95$ in the region $\rho\simeq a$.

The graphs for the two models are similar, especially for the axial component in the regions not too close to the wires. This similarity justifies the use of the simpler model discussed in Sec. II A as an acceptable approximation for the thick coil if the demands on accuracy are not too restrictive.

Note that our models exclude the regions close to the wires up to the order of magnitude of their diameter, where the magnetic field is affected by the periodicity, shape, and internal structure of the wires.

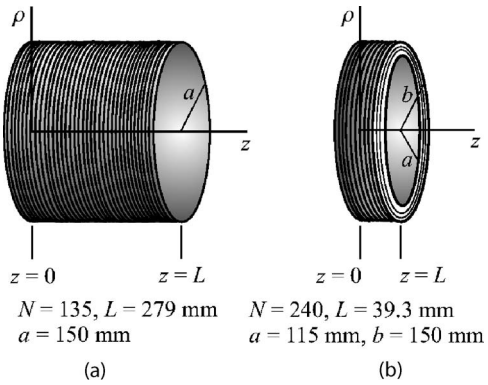

Fig. 4. The real coils used in our laboratory experiment to measure magnetic fields: (a) single-layer solenoid, (b) cylindrical thick coil.

III. MEASUREMENTS

A coil was connected in series with an ammeter and a regulated dc power supply serving as a current source up to 9 A to create magnetic fields strong enough to be detected by a commercially available Hall effect probe. The sensor was linked by a converting unit to a computer with software for data processing and display. All measurements were done with a maximum sensitivity of 0.1 G.

To ensure accurate and reliable measurements of the magnetic field at different points in space inside and outside the coils, we have to know the location of the probe in a well defined coordinate system. For this purpose a set of movable Plexiglas™ discs of different radii were mounted vertically on a horizontal brass rod which coincided with the z axis and was linearly calibrated for the coordinate z. The cylindrical coordinates ρ and ϕ were defined by the corresponding grids marked on the discs. The reproducibility of the measured data was tested during the experiment.

The coils used in our experiment are depicted in Fig. 4. Their position and geometric features will be referenced from the end of the coil. L is the length of the coil and a and b its inner and outer radius, respectively.

The single-layer solenoid used in our experiment [Fig. 4(a)] was hand wound on a 30-cm-diam hard plastic tube consisting of 135 single-layer turns of copper wire of diameter equal to 2.1 mm. The applied currents ranged between 3 and 9 A.

The cylindrical thick coil [Fig. 4(b)] was obtained by detaching a Helmholtz pair. It was made from 240 multilayer (16×15) turns of wire of diameter equal to 2.3 mm. The measured magnetic fields were produced by currents of 1–5 A.

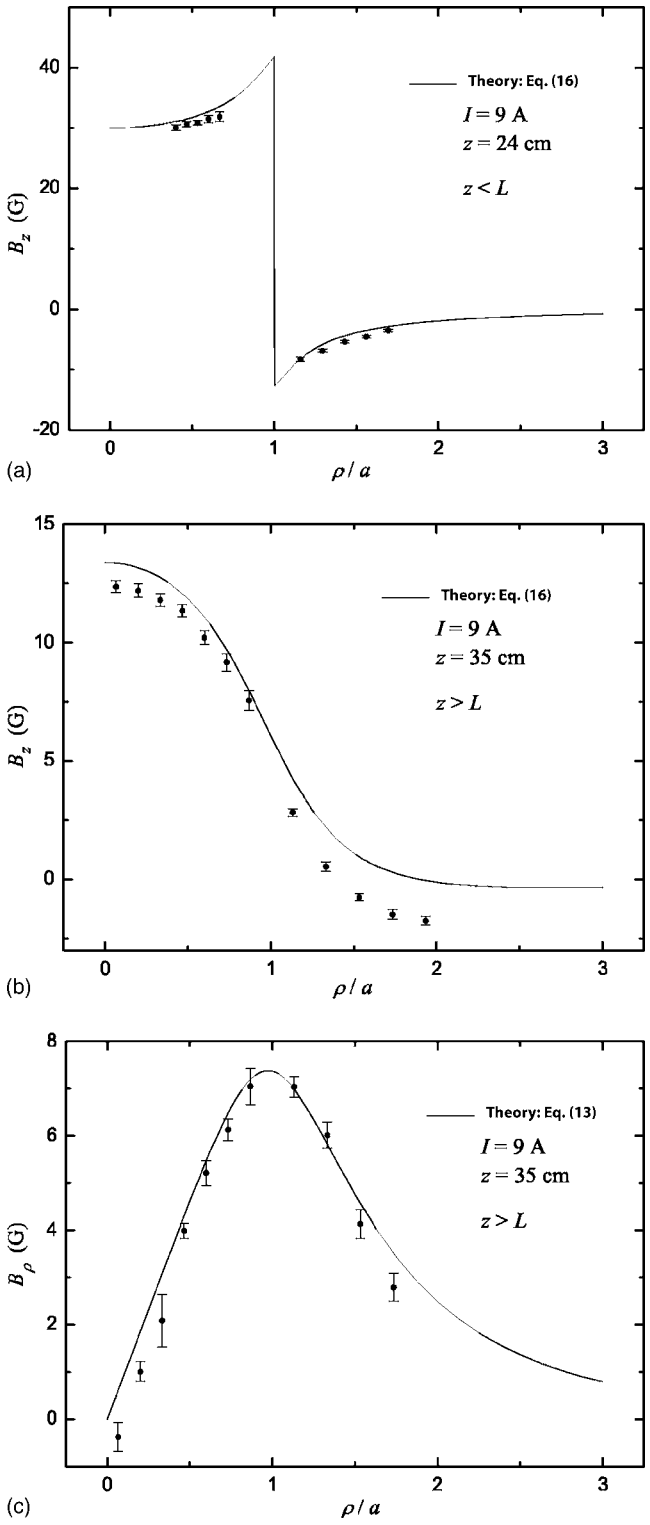

Fig. 5. The axial and radial magnetic field components, Eqs. (13) and (16), inside and outside the single-layer solenoid as a function of the radial distance from the axis reduced to the inner radius.

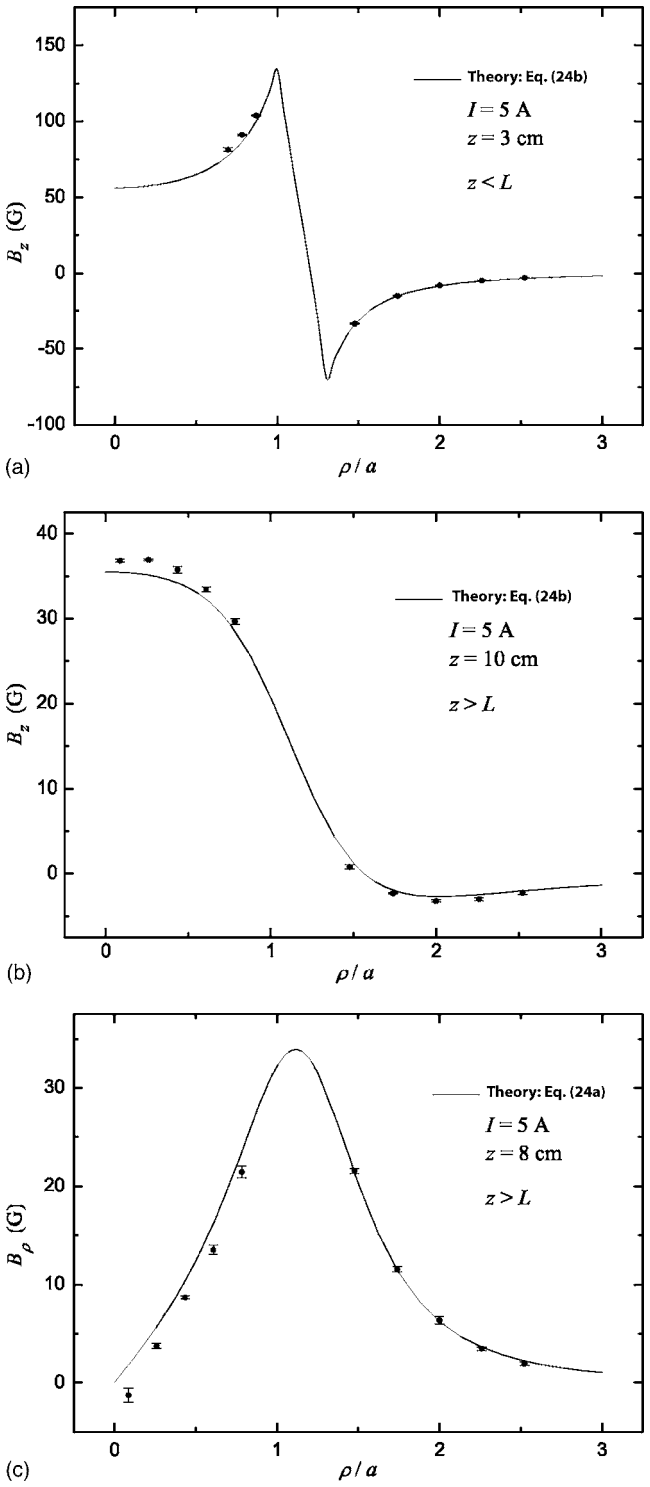

Fig. 6. Same as Fig. 5 for the cylindrical thick coil. The measurements are compared with Eq. (24).

The axial and radial magnetic field components were measured by the corresponding orientations of the probe. Each magnetic field value was averaged over ten measurements recorded during 10 s in 1 s intervals.

Results. The complete set of our results for both coils is available.[23] Examples of plots for given values of the axial distance z and current I, representing magnetic field components as a function of the radial distance from the axis reduced to the radius of the coil, are given for both types of coils in Figs. 5 and 6. The vertical bars represent the field variations caused by current changes during 10 s intervals. Examples of the measured magnetic field components of the single-layer solenoid are plotted in Fig. 5 together with our calculated curves, Eqs. (13) and (16), which are represented by a full line. The same is done in Fig. 6 for the thick coil

where the results of calculations given in Eq. (24) were adopted as the best approximation for this type of coil.

To compare the theoretical and experimental results, different effects should be taken into account. The theoretical curves were determined for fixed current values while the experimental points correspond to currents averaged over 10 s intervals. These average values were also changing in time, probably due to the heating of the wire and could not be readjusted to the same fixed value.

Still better agreement of theory and experiment could be attained by taking account of other effects, such as interference fields from the nearby conductors and electrical devices, asymmetries in the experimental apparatus, and the Earth's magnetic field. We have tested these effects by measuring the magnetic fields outside a straight conductor under identical laboratory circumstances and found that the direction of the vertical shift of the measured values with respect to the theoretical prediction depends on the direction of the applied current. The shift varied between 0.5 and 1 G, which exceeds the contribution of the Earth's field, which has a horizontal component of 0.22 G at our latitude,[24] and would affect the axial magnetic field. The angle between the z axis and the N-S direction equal to 16° makes this contribution insignificantly smaller, by 0.01 G, which is not measurable in our experiment. The influence of the Earth's field on the radial component can be neglected because our measurements were carried out in the horizontal plane.

IV. CONCLUSION

The comparison of theory and experiment of a physical phenomenon, like the magnetic field in our example, is valuable pedagogically because it facilitates students' comprehension of the subject. The coil, as the basic element for producing a homogeneous magnetic field due to a current, is good for demonstrations and simple experiments and the necessary theoretical expression can be found straightforwardly in a few steps starting from Ampere's law. More realistic field configurations can be produced by commonly used coil designs (for example, Helmholtz coils).

The magnetic field in more realistic configurations can be calculated much easier numerically from the beginning. The analytical expressions for the two coil configuration derived in this paper can be used to test the numerical methods developed for more complex coil designs used, for example, in various nuclear devices (NMR), accelerators (magnetic lensing, beam bending), isotope separators, mass spectrometers, and thermonuclear installations (magnetic confinement).

ACKNOWLEDGMENTS

Our thanks are due to Mirjana Turina, Ljubomir Špirić, and Tomislav Pernjak for their help in carrying out the measurements.

APPENDIX: INTEGRALS

Equations (A1) and (A2) were used in deriving the expressions for the radial magnetic field component, Eq. (13), and Eqs. (A3) and (A4) were applied to the calculation of the axial component of the magnetic field, Eq. (16), for the cylindrical surface current (Sec. II A). Equation (A5) was used in the calculation of the magnetic field of the cylindrical shell volume current, Eq. (24), in Sec. II B. Integrals (A1)–(A5) are given in Gradshteyn and Ryzhik[25] and the integral (A5) was calculated by use of MATHEMATICA:

$$\int_0^\infty dx J_1(\beta x) J_1(\gamma x) e^{-\alpha x} = \frac{1}{\pi\sqrt{\beta\gamma}} Q_{1/2}\left(\frac{\alpha^2+\beta^2+\gamma^2}{2\beta\gamma}\right), \tag{A1}$$

$$Q_{1/2}(x) = \frac{\Gamma\left(\frac{3}{2}\right)\Gamma\left(\frac{1}{2}\right)}{2^{3/2}\Gamma(2)} x^{-3/2} F\left(\frac{5}{4},\frac{3}{4};2;\frac{1}{x^2}\right). \tag{A2}$$

$$\int_0^\infty dx J_1(\alpha x) J_0(\beta x) = \begin{cases} a^{-1}, & \rho < a \\ 0, & \rho > a, \end{cases} \tag{A3}$$

$$\int_0^\infty dx J_\nu(\beta x) x^{\mu-1} e^{-\alpha x} = \left(\frac{\beta}{2\alpha}\right)^\nu \frac{\Gamma(\nu+\mu)}{\alpha^\mu \Gamma(\nu+1)} \times F\left(\frac{\mu+\nu}{2},\frac{\mu+\nu+1}{2};\nu+1;-\frac{\beta^2}{\alpha^2}\right), \tag{A4}$$

$$\int_a^b dx J_1(\gamma x) x = \frac{\pi}{2\gamma}[-aJ_1(\gamma a)H_0(\gamma a) + bJ_1(\gamma b)H_0(\gamma b) + aJ_0(\gamma a)H_1(\gamma a) - bJ_0(\gamma b)H_1(\gamma b)]. \tag{A5}$$

[a]Electronic mail: dubravka.karuza-kotnik@ri.htnet.hr

[1] David J. Griffiths, *Introduction to Electrodynamics* (Prentice Hall, Upper Saddle River, NJ, 1999), 3rd ed., pp. 227–228.
[2] B. B. Dasgupta, "Magnetic field due to a solenoid," Am. J. Phys. **52**, 258 (1984).
[3] V. Namias, "On the magnetic field due to a solenoid of arbitrary cross section," Am. J. Phys. **53**, 588 (1985).
[4] K. Fillmore, "Magnetic field of a noncircular solenoid," Am. J. Phys. **53**, 782–783 (1985).
[5] O. Espinosa and V. Slusarenko, "The magnetic field of an infinite solenoid," Am. J. Phys. **71**(9), 953–954 (2003).
[6] Edward M. Purcell, *Electricity and Magnetism* (McGraw-Hill, New York, 1985), 2nd ed., pp. 226–231.
[7] John D. Jackson, *Classical Electrodynamics* (Wiley, New York, 1999), 3rd ed., pp. 225–227.
[8] C. Chia and Y. Wang, "The magnetic field along the axis of a long finite solenoid," Phys. Teach. **40**, 288–289 (2002).
[9] J. Farley and R. H. Price, "Field just outside a long solenoid," Am. J. Phys. **69**, 751–754 (2001).
[10] G. V. Brown and L. Flax, "Superposition of semi-infinite solenoids for calculating magnetic fields of thick solenoids," J. Appl. Phys. **35**, 1764–1767 (1964).
[11] R. H. Jackson, "Off-axis expansion solution of Laplace's equation. Application to accurate and rapid calculation of coil magnetic fields," IEEE Trans. Electron Devices **46**, 1050–1062 (1999).
[12] J. T. Conway, "Exact solutions for the magnetic fields of axisymmetric solenoids and current distributions," IEEE Trans. Magn. **37**, 2977–2988 (2001).
[13] Daryl W. Preston and Eric R. Deitz, *The Art of Experimental Physics* (Wiley, New York, 1991), pp. 121–125, 303–315.
[14] C. G. Deacon and H. C. Clarke, "Use of a linear offset Hall effect transducer in student laboratory experiments to measure magnetic fields," Am. J. Phys. **61**, 947–948 (1993).
[15] D. Bishir, "A simple demonstration of the magnetic field of a solenoid," Am. J. Phys. **64**, 1525 (1996).

[16] H. B. Dwight, "The magnetic field of a circular cylindrical coil," Philos. Mag. **11**, 948–957 (1931).
[17] M. W. Garrett, "Axially symmetric systems for generating and measuring magnetic fields. Part I," J. Appl. Phys. **22**, 1091–1107 (1951).
[18] A. I. Rusinov, "High precision computation of a solenoid magnetic fields by Garett's methods," IEEE Trans. Magn. **30**, 2685–2688 (1994).
[19] Philip M. Morse and Herman Feshbach, *Methods of Theoretical Physics, Part II* (McGraw-Hill, New York, 1953), p. 1263.
[20] The common notation for the Gauss hypergeometric function has the form ${}_2F_1(a,b;c;\xi)$ where a, b, and c are parameters.
[21] MATHEMATICA, ⟨http://www.wolfram.com⟩.
[22] The common notation for Struve functions is $\mathbf{H}_n(\xi)$.
[23] See EPAPS Document No. E-AJPIAS-74-021606 for the plots and tables for all measurements. This document can be reached via a direct link in the online article's HTML reference section or via the EPAPS homepage (http://www.aip.org/pubservs/epaps.html).
[24] The Earth's magnetic field for different locations can be determined at ⟨http://www.ngdc.noaa.gov/seg/geomag/magfield.shtml⟩.
[25] I. S. Gradshteyn and I. M. Ryzhik, *Table of Integrals, Series, and Products* (Academic, New York, 2000), 6th ed..

DIRAC EQUATION

"[Paul] Dirac's equation can be written in one line:

$$\frac{ih}{2\pi}\frac{\partial|\psi>}{\partial t} = (c\vec{u}\cdot\vec{P} + \beta mc^2)|\psi> .$$

From the solution of this little equation come details about the hydrogen atom, the spin of the electron, and the existence of anti-matter. Poets bring us fresh insights with the right sequence of words, Dirac brought us fresh insights with the right sequence of symbols."

John S. Rigden, *Hydrogen: The Essential Element* (Cambridge University Press, Cambridge, Massachusetts, 2005), p. 94.